JACS
JOURNAL OF THE AMERICAN CHEMICAL SOCIETY
Communication
pubs.acs.org/JACS

Reaction Mechanisms for the Electrochemical Reduction of CO_2 to CO and Formate on the Cu(100) Surface at 298 K from Quantum Mechanics Free Energy Calculations with Explicit Water

Tao Cheng, Hai Xiao, and William A. Goddard III*

Joint Center for ArtificialPhotosynthesis (JCAP) and Materials and Process Simulation Center(MSC) (MC139-74), California Institute ofTechnology, Pasadena, California 91125, United States

Supporting Information

ABSTRACT: Copper is the only elemental metal that reduces a significant fraction of CO_2 to hydrocarbons and alcohols, but the atomistic reaction mechanism that controls the product distributions is not known because it has not been possible to detect the reaction intermediates on the electrode surface experimentally, or to carry out Quantum Mechanics (QM) calculations with a realistic description of the electrolyte (water). Here, we carry out QM calculations with an explicit description of water on the Cu(100) surface (experimentally shown to be stable under CO_2 reduction reaction conditions) to examine the initial reaction pathways to form CO and formate ($HCOO^-$) from CO_2 through free energy calculations at 298 K and pH 7. We find that CO formation proceeds from physisorbed CO_2 to chemisorbed CO_2 ($*CO_2^{\delta-}$), with a free energy barrier of $\Delta G^{\ddagger}$ = 0.43 eV, the rate-determining step (RDS). The subsequent barriers of protonating $*CO_2^{\delta-}$ to form COOH* and then dissociating COOH* to form *CO are 0.37 and 0.30 eV, respectively. $HCOO^-$ formation proceeds through a very different pathway in which physisorbed CO_2 reacts directly with a surface H* (along with electron transfer), leading to $\Delta G^{\ddagger}$ = 0.80 eV. Thus, the competition between CO formation and $HCOO^-$ formation occurs in the first electron-transfer step. On Cu(100), the RDS for CO formation is lower, making CO the predominant product. Thus, to alter the product distribution, we need to control this first step of CO_2 binding, which might involve controlling pH, alloying, or changing the structure at the nanoscale.

In order to reduce the carbon footprint and to convert renewable energy production (from wind or solar) into stable chemical forms, we need an economical process for the CO_2 reduction reaction (CO_2RR). Copper is the only elemental metal that electrochemically catalyzes formation of significant amounts of hydrocarbons,[1] but it requires a high overpotential (0.9 V) for a reasonable current,[2] and it leads to a mixture of major products (including hydrogen gas, ethylene, and methane) plus small amounts of other C_2's, C_3's, and oxygenates.[3,4] Due to its unique ability to catalyze hydrocarbon formation, Cu is a prototype to determine and validate the mechanism of hydrocarbon formation, to serve as the basis for designing new catalysts that increase product selectivity and rates while simultaneously lowering overpotentials. A number of excellent reviews summarize previous research associated with CO_2RR on Cu.[5−7]

The product distribution of CO_2 reduction depends on the applied potential.[1−3,8] For polycrystalline Cu at pH 6.8, CO formation starts at −0.90 V (NHE) [or −0.50 V (RHE)] and predominates at potentials less negative than −1.2 V (NHE) [or −0.8 V (RHE),] where it competes with formate ($HCOO^-$) formation. CO, formed as an intermediate from CO_2, is adsorbed on the Cu electrode, interfering with the cathodic hydrogen evolution reaction (HER). At potentials more negative than −1.3 V (NHE) [or −0.9 V (RHE)], the adsorbed CO is reduced to hydrocarbons (methane and ethylene) and alcohols, with a decrease in CO Faradaic efficiency. Indeed, electroreduction of CO leads to product distributions and onset potentials very similar to those of CO_2RR.[6,7,9,10] Therefore, Quantum Mechanics (QM) studies on the mechanism of CO_2RR have focused mainly on the CO reduction reaction (CORR) mechanism to predict intermediates involved in the formation of CH_4 and C_2H_4.[11−19]

There have been several previous QM calculations of CO_2RR on Cu,[11,13,18,20] but none of these calculations included the liquid/electrode interface. Since this interface is expected to have a dramatic direct influence on the thermodynamics and kinetics of chemical reactions, we consider it essential to include multiple layers of explicit water to properly describe reactions at the catalyst−solvent interface. In this Communication, we report the first such calculations of QM-based reaction molecular dynamics (MD) of CO_2RR using five layers of fully flexible QM water. We evaluate the MD forces using QM forces (often termed ab initio MD or AIMD) and use enhanced sampling methods[21,22] [metadynamics[23,24] and constrained MD[25] (blue moon ensemble)] at 298 K to obtain the free energy (FE) reaction barriers[22−27] for various possible reaction pathways in the reduction of CO_2 to CO and formate on the Cu(100) surface, which has been shown experimentally to be the dominant surface for polycrystalline Cu under electrochemical conditions for CO_2RR.[28]

To describe the water/Cu(100) interface, we included five explicit layers of water molecules (48 molecules, 1.21 nm thick) on a 4×4 Cu (100) surface slab (three layers) with an area of 1.02 nm^2. To equilibrate the waters interacting at this interface,

Received: August 17, 2016
Published: October 11, 2016

DOI: 10.1021/jacs.6b08534
J. Am. Chem. Soc. 2016, 138, 13802−13805

we carried out 2 ns of reactive molecular dynamics (RMD) simulations using the ReaxFF reactive force field for Cu and H_2O.[29] Starting from this well-equilibrated interface, we carried out independent 10 ps QM RMD simulations for a number of reaction processes at 298 K. Then, we used metadynamics[23,24] and thermodynamic integration[25] to calculate the FE barriers for each of these reaction steps (each result was averaged over three independent calculations).[22−27]

We calculate the potential of zero charge (PZC) of Cu(100) in contact with explicit water to be 3.61 eV, which corresponds to −0.38 V (RHE) (3.61 − 4.40 + 0.0592 × 7 = −0.38 V), close to the onset potential [−0.50 V (RHE)] of CO production at pH 6.8.[2] Adsorption of reactive species can slightly change the PZC from 3.58 to 3.75 eV [details are shown in Table S2 in the Supporting Information (SI)]. We believe that this model of QM with explicit treatment of the water dynamics at 298 K provides a good description of the reaction kinetics.

Both Eley−Rideal (ER) and Langmuir−Hinshelwood (LH) mechanisms were considered for each reaction. In ER, H_2O and e^- are used in the reduction reaction (e^- is used implicitly). In LH, one surface hydrogen (H*) is used in the reduction reaction, which corresponds to the low coverage condition (0.1 ML) in experiment.[30] For LH, the formation of H* implicitly involves either H_3O^+ or OH^-, so that both the reaction barrier ($\Delta G^{\ddagger}$) and the energy (ΔG) are pH dependent. At pH 6.8, the $\Delta G^{\ddagger}$ and ΔG of reactions via LH are corrected by 0.4 eV (0.0592 × 6.8) to compare with the ER reactions.

To examine CO_2RR, we inserted one CO_2 molecule into the third layer and equilibrated with QM for 20 ps. We found that this CO_2 molecule diffused into the first layer, attaining an average distance of 3.67 Å between the center of mass (COM) of CO_2 and the first layer of Cu, as shown in Figure 1A,E. This indicates that the CO_2 binds only very weakly to Cu(100), in contrast to CO, which chemisorbs on the electrode surface strongly enough to suppress HER for potentials less negative than −0.4 eV (RHE).[2]

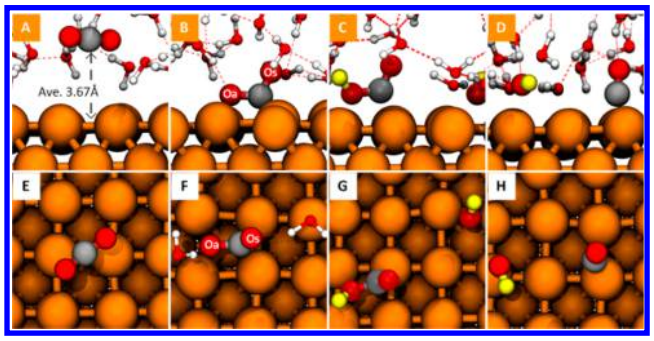

Figure 1. Snapshots (side view and top view) of reactive intermediates in the reduction of CO_2 to form CO based on QM RμD simulations at 298 K and pH 7. The colors are Cu in orange, C in gray, O in red, and H in yellow (involved in reaction) or white (in solvent). Hydrogen bonds (HBs) are indicated as red dashed lines. (A) and (E) show physisorbed CO_2 on the Cu(100) surface. The average distance between the CO_2 center of mass and first layer of Cu is 3.67 Å. (B) and (F) show chemisorbed $*CO_2^{\delta-}$ on the Cu(100) surface. The two C−O bonds have lengths of $r(C-O_a)$ = 1.33 Å and $r(C-O_s)$ = 1.29 Å. Neighboring water molecules form one HB to O_a of $*CO_2^{\delta-}$ and one HB to O_s. The free energy barrier is $\Delta G^{\ddagger}$ = 0.43 eV for forming this state from the one in (A) and (E). (C) and (G) show *COOH. The free energy barrier is $\Delta G^{\ddagger}$ = 0.37 eV for forming *COOH + $*OH^-$ from the state in (B) and (F) plus H_2O*. (D) and (H) show *CO and *OH formed by dissociating the *COOH from the state in (C) and (G). The free energy barrier is $\Delta G^{\ddagger}$ = 0.30 eV. This reaction is assisted by the formation of additional HBs to the products *OH and *CO.

In order to obtain the FE reaction barriers in metadynamics, we apply a bias force to the COM of CO_2 that drives the CO_2 toward the Cu(100) surface. At a distance of 1.62 Å between the CO_2 COM and the first layer of Cu, we find that a chemisorbed bent $*CO_2^{\delta-}$ forms on the surface, as shown in Figure 1B. This adsorption geometry of $*CO_2^{\delta-}$ has not yet been observed experimentally. However, several structures have been postulated for the $*CO_2^{\delta-}$−metal complex, including carbon coordination, oxygen coordination (one site or two sites), and mixed coordination (one site of two sites).[31,32] Our QM studies find that mixed coordination with two sites is the most favorable, leading to the $*CO_2^{\delta-}$ adsorption configuration shown in Figure 1B. In this configuration, one C−O bond (C−O_a) is parallel with the Cu surface, while the other CO bond (C−O_s) is tilted by 67.5° toward solvent. (Here "a" is for absorbed and "s" is for solvent.) The lengths of these two CO bonds are similar: $r(C-O_a)$ = 1.33 Å and $r(C-O_s)$ = 1.29 Å. The average angle between these two bonds is 112.5°. The top view of $*CO_2^{\delta-}$ (Figure 1F) shows that both C and O_a are at 2-fold bridge sites spanning the 4-fold hollow of Cu(100). Therefore, $*CO_2^{\delta-}$ occupies two surface sites upon adsorption.

The FE barrier ($\Delta G^{\ddagger}$) from physisorbed CO_2 to $*CO_2^{\delta-}$ is 0.43 eV. This $*CO_2^{\delta-}$ species is stabilized by the water solvent hydrogen bond (HB) network. One water molecule donates a hydrogen toward forming a HB to O_a, while a second water forms a HB to O_s, as shown in Figure 1B,F. The average lengths of these two HBs are 1.73 Å [$r(O-H\cdots O_a)$] and 1.85 Å [$r(O-H\cdots O_s)$], which compare well to the value of 1.97 Å in pure solvent.[33] Although physisorbed CO_2 is 0.39 eV more stable than chemisorbed CO_2 ($*CO_2^{\delta-}$), we find that $*CO_2^{\delta-}$ is kinetically stable over a 20 ps brute force AIMD simulation, with no tendency to return to the physisorbed CO_2. This is because the HB network restructures to adapt to either CO_2 structure. Therefore, we consider that $*CO_2^{\delta-}$ is the first reactive intermediate (not just a transition state as proposed previously)[20] in the electrochemical reduction of CO_2.

We next used QM reactive metadynamics (RμD) to examine the barrier for adding a hydrogen from H_2O to O_a of $*CO_2^{\delta-}$ to form *cis*-*COOH (*COO_aH) plus OH*. We find that $\Delta G^{\ddagger}$ = 0.37 eV via an ER mechanism, as shown in Figure 1C,G. An alternative mechanism would be to add a hydrogen to O_s, which results in *trans*-*COOH (*COO_sH), but this has $\Delta G^{\ddagger}$ = 0.40 eV, so the rate is lower by a factor of 3.1 at 298 K. This slightly higher barrier for forming *trans*-*COO_aH may by attributed to the same reason that the bond length of $r(C-O_s)$ is 0.04 Å shorter than $r(C-O_a)$. We also considered forming *COO_aH via the LH mechanism, but this leads to a large $\Delta G^{\ddagger}$ = 1.54 eV, so that the rate is lower by a factor of 4×10^{19} at 298 K. Therefore, **COOH formation proceeds via ER.* This is consistent with our previous studies of CORR, where we find that ER reactions are always favored over LH when adding hydrogen to oxygen.[15]

The final step of CO formation is dehydroxylation of *COOH to form CO plus OH*. Here the QM RμD leads to $\Delta G^{\ddagger}$ = 0.30 eV via ER, as shown in Figure 1D,H. This produces *CO chemisorbed on Cu(100). We calculated the binding energy of CO* on the surface in solvent by moving CO into the solvent. This process is purely uphill (no barrier associated), with FE difference ΔG = 0.90 eV. This is higher than the values for *CHO formation ($\Delta G^{\ddagger}$ = 0.55 eV at pH 0

DOI: 10.1021/jacs.6b08534
J. Am. Chem. Soc. 2016, 138, 13802−13805

and 0.96 eV at pH 7)[15,34] or *CO dimerization ($\Delta G^{\ddagger}$ = 0.69 eV at pH 7) we reported previously.[34] Therefore, on Cu(100), an increased potential leads *CO to undergo electrochemical hydrogenation reduction to hydrocarbons without desorbing from the surface.

Summarizing our FE calculations, we find the following reaction pathway for CO formation from CO_2:

$$CO_2(aq) \xrightarrow[0.43\ eV]{\delta e^-} *CO_2^{\delta-} \xrightarrow[0.37\ eV]{H_2O+(1-\delta)e^-} *COOH \xrightarrow[0.30\ eV]{e^-} *CO + OH^- \quad (1)$$

Here, the first step is from physisorbed CO_2 to chemisorbed $*CO_2^{\delta-}$, with $\Delta G^{\ddagger}$ = 0.43 eV. This asymmetric chemisorbed CO_2 intermediate is very similar to the intermediate proposed to be involved in the water−gas shift reaction at the interface of a Cu(111)/ceria nanoparticle.[35]

Experimentally, $HCOO^-$ formation has been thought to compete with CO formation.[2,3] One proposed pathway of $HCOO^-$ formation is by adding hydrogen to carbon of $*CO_2^{\delta-}$ either via ER reaction or LH reaction. However, for this process we find that $\Delta G^{\ddagger}$ = 1.12 eV via ER and $\Delta G^{\ddagger}$ = 0.99 eV via LH, so neither of these reactions can be responsible. Both are much higher than the $\Delta G^{\ddagger}$ = 0.37 eV for *COOH formation. Peterson et al.[11] proposed that HCOOH might be formed on Cu(211) through an alternate reaction pathway involving *COOH.[11] However, for Cu(100) we find that the FE barrier for $HCOO^-$ formation is 1.06 eV (HOOH directly dissociate into $HCOO^-$ at pH 7), which is much higher than the 0.30 eV barrier for *CO formation from *COOH. Therefore, on Cu(100), *$CO_2^{\delta-}$ leads only to CO formation, with no formation of $HCOO^-$.*

Instead, we have found an alternative (not previously proposed) reaction pathway for $HCOO^-$ formation. This is through a surface H* reacting with physisorbed CO_2. In this reaction pathway, CO_2 need not be first activated by the metal surface. Instead, the physisorbed CO_2 reacts directly with surface H* along with one electron transfer to form $HCOO^-$. This has $\Delta G^{\ddagger}$ = 0.80 eV, which is much lower than $HCOO^-$ formation via $*CO_2^{\delta-}$ (0.99 eV via LH or 1.22 eV via ER). Snapshots of the reaction trajectories are shown in Figure 2. Therefore, we conclude that *the major reaction contributing to $HCOO^-$ formation is the one-step direct reduction via physisorbed CO_2 reacting with H**, as follows:

$$CO_2(aq) \xrightarrow[0.80\ eV]{H^*+e^-} HCOO^-(aq) \quad (2)$$

These results explain why $HCOO^-$ production always competes with HER, since both need H*.[7] Our mechanism is also consistent with the experimental observation that electrodes such as Hg, Cd, Pb, Tl, In, and Sn,[36] that have high hydrogen overpotential for HER with weak adsorption of hydrogen, also have a high overpotential for CO_2 reduction to $*CO_2^{\delta-}$ (hence a weak adsorption/stabilization of $*CO_2^{\delta-}$), so that they produce predominantly formate in aqueous CO_2 electrolysis.

Summarizing, we used QM RμD FE calculations to predict the reaction barriers for the elementary reactions in CO_2 electrochemical reduction, while including five layers of explicit water solvent. We find that *the lowest kinetic reaction pathways for CO formation and for $HCOO^-$ formation are quite distinct*, as shown in Scheme 1 (details are in SI).

Thus, the competition between CO formation and $HCOO^-$ formation occurs in the first electron reduction step:

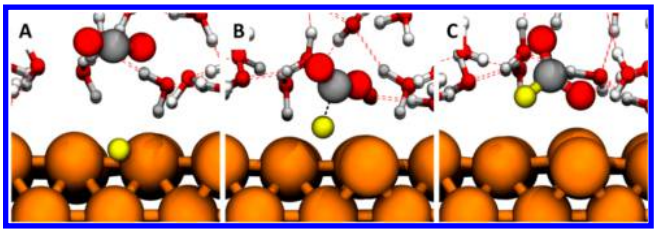

Figure 2. Snapshots of the reactive intermediates in the formate formation pathway from QM RμD simulations at 298 K and pH 7. The colors are Cu in orange, C in gray, O in red, and H in yellow (involved in reaction) or white (in water). Hydrogen bonds (HBs) are denoted as red dashed lines. (A) Initial state (CO_2 + H*). (B) Transition state (TS). (C) Final state ($HCOO^-$). $\Delta G^{\ddagger}$ = 0.80 eV from (A) to (B). The C−H forming bond is 1.56 Å in (B) and 1.10 Å in (C). Notice that several HBs to solvent water play an important role in the energetics.

Scheme 1. Most Favorable Kinetic Pathways for the Electrochemical Reduction of CO_2 to *CO and Formate ($HCOO^-$) in Water Solvent at pH 7

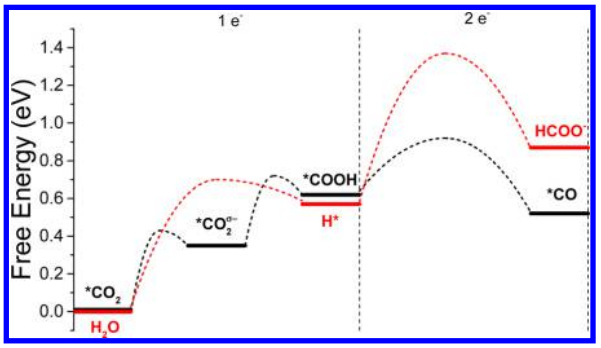

- Chemisorption to form $*CO_2^{\delta-}$ leads to CO formation.
- CO_2 direct reduction by surface H* leads to $HCOO^-$ formation.

Since the CO and formate products involve very different reaction mechanisms, it should be possible to control which one dominates by modifying either the binding energy of CO_2 or the formation energy for H*, which in turn would alter the ratio of CO production to $HCOO^-$ production. This might be achievable by controlling pH, by alloying, by designing new nanoscale catalysts, or by modifying the properties of the electrolyte.

Having validated the power of explicit solvent QM RμD calculations for determining the mechanisms and free energy barriers for electrochemical reduction of CO_2, we can anticipate that such calculations will be most powerful for designing new catalysts to be selective and active for CO_2 reduction to valuable products.

■ ASSOCIATED CONTENT

Supporting Information

The Supporting Information is available free of charge on the ACS Publications website at DOI: 10.1021/jacs.6b08534.

Simulation details, details of free energy calculations, definition of collective variables for each elementary reactions, and constant potential corrections (PDF)

■ AUTHOR INFORMATION

Corresponding Author

*wag@wag.caltech.edu

DOI: 10.1021/jacs.6b08534
J. Am. Chem. Soc. 2016, 138, 13802−13805

Notes

The authors declare no competing financial interest.

■ ACKNOWLEDGMENTS

This work was fully supported by the Joint Center for Artificial Photosynthesis, a DOE Energy Innovation Hub, supported through the Office of Science of the U.S. Department of Energy under Award No. DE-SC0004993. We thank Mr. Yufeng Huang, Dr. Ravishankar Sundararaman, Dr. Robert J. Nielsen, and Prof. Manuel P. Soriaga for helpful discussions. The calculations were carried out mostly on the Zwicky (Caltech) astrophysics computing system [using funding from NSF (CBET 1512759)], with some on NERSC.

■ REFERENCES

(1) Hori, Y.; Kikuchi, K.; Suzuki, S. *Chem. Lett.* **1985**, *14*, 1695.
(2) Hori, Y.; Murata, A.; Takahashi, R. *J. Chem. Soc., Faraday Trans. 1* **1989**, *85*, 2309.
(3) Kuhl, K. P.; Cave, E. R.; Abram, D. N.; Jaramillo, T. F. *Energy Environ. Sci.* **2012**, *5*, 7050.
(4) Schouten, K. J. P.; Kwon, Y.; van der Ham, C. J. M.; Qin, Z.; Koper, M. T. M. *Chem. Sci.* **2011**, *2*, 1902.
(5) Kortlever, R.; Shen, J.; Schouten, K. J. P.; Calle-Vallejo, F.; Koper, M. T. M. *J. Phys. Chem. Lett.* **2015**, *6*, 4073.
(6) Hori, Y. In *Modern Aspects of Electrochemistry*; Vayenas, C., White, R., Gamboa-Aldeco, M., Eds.; Springer: New York, 2008; Vol. *42*, p 89.
(7) Gattrell, M.; Gupta, N.; Co, A. *J. Electroanal. Chem.* **2006**, *594*, 1.
(8) Hori, Y.; Takahashi, I.; Koga, O.; Hoshi, N. *J. Mol. Catal. A: Chem.* **2003**, *199*, 39.
(9) Hori, Y.; Murata, A.; Takahashi, R.; Suzuki, S. *J. Am. Chem. Soc.* **1987**, *109*, 5022.
(10) Hori, Y.; Takahashi, R.; Yoshinami, Y.; Murata, A. *J. Phys. Chem. B* **1997**, *101*, 7075.
(11) Peterson, A. A.; Abild-Pedersen, F.; Studt, F.; Rossmeisl, J.; Norskov, J. K. *Energy Environ. Sci.* **2010**, *3*, 1311.
(12) Calle-Vallejo, F.; Koper, M. T. M. *Angew. Chem., Int. Ed.* **2013**, *52*, 7282.
(13) Nie, X.; Esopi, M. R.; Janik, M. J.; Asthagiri, A. *Angew. Chem., Int. Ed.* **2013**, *52*, 2459.
(14) Schouten, K. J. P.; Calle-Vallejo, F.; Koper, M. T. M. *Angew. Chem., Int. Ed.* **2014**, *53*, 10858.
(15) Cheng, T.; Xiao, H.; Goddard, W. A. *J. Phys. Chem. Lett.* **2015**, *6*, 4767.
(16) Montoya, J. H.; Shi, C.; Chan, K.; Nørskov, J. K. *J. Phys. Chem. Lett.* **2015**, *6*, 2032.
(17) Goodpaster, J. D.; Bell, A. T.; Head-Gordon, M. *J. Phys. Chem. Lett.* **2016**, *7*, 1471.
(18) Luo, W.; Nie, X.; Janik, M. J.; Asthagiri, A. *ACS Catal.* **2016**, *6*, 219.
(19) Xiao, H.; Cheng, T.; Goddard, W. A.; Sundararaman, R. *J. Am. Chem. Soc.* **2016**, *138*, 483.
(20) Nie, X.; Luo, W.; Janik, M. J.; Asthagiri, A. *J. Catal.* **2014**, *312*, 108.
(21) Voter, A. F.; Montalenti, F.; Germann, T. C. *Annu. Rev. Mater. Res.* **2002**, *32*, 321.
(22) Ensing, B.; De Vivo, M.; Liu, Z.; Moore, P.; Klein, M. L. *Acc. Chem. Res.* **2006**, *39*, 73.
(23) Laio, A.; Parrinello, M. *Proc. Natl. Acad. Sci. U. S. A.* **2002**, *99*, 12562.
(24) Iannuzzi, M.; Laio, A.; Parrinello, M. *Phys. Rev. Lett.* **2003**, *90*, 238302.
(25) Fleurat-Lessard, P.; Ziegler, T. *J. Chem. Phys.* **2005**, *123*, 084101.
(26) Laio, A.; Rodriguez-Fortea, A.; Gervasio, F. L.; Ceccarelli, M.; Parrinello, M. *J. Phys. Chem. B* **2005**, *109*, 6714.
(27) Ensing, B.; Laio, A.; Parrinello, M.; Klein, M. L. *J. Phys. Chem. B* **2005**, *109*, 6676.
(28) Kim, Y.-G.; Baricuatro, J. H.; Javier, A.; Gregoire, J. M.; Soriaga, M. P. *Langmuir* **2014**, *30*, 15053.
(29) van Duin, A. C. T.; Bryantsev, V. S.; Diallo, M. S.; Goddard, W. A.; Rahaman, O.; Doren, D. J.; Raymand, D.; Hermansson, K. *J. Phys. Chem. A* **2010**, *114*, 9507.
(30) Abd Elhamid, M. H.; Ateya, B. G.; Weil, K. G.; Pickering, H. W. *J. Electrochem. Soc.* **2000**, *147*, 2148.
(31) Freund, H. J.; Messmer, R. P. *Surf. Sci.* **1986**, *172*, 1.
(32) Freund, H. J.; Roberts, M. W. *Surf. Sci. Rep.* **1996**, *25*, 225.
(33) Legon, A. C.; Millen, D. J. *Chem. Soc. Rev.* **1987**, *16*, 467.
(34) Cheng, T.; Xiao, H.; Goddard, W. A. Submitted for publication, 2016.
(35) Graciani, J.; Mudiyanselage, K.; Xu, F.; Baber, A. E.; Evans, J.; Senanayake, S. D.; Stacchiola, D. J.; Liu, P.; Hrbek, J.; Sanz, J. F.; Rodriguez, J. A. *Science* **2014**, *345*, 546.
(36) Todoroki, M.; Hara, K.; Kudo, A.; Sakata, T. *J. Electroanal. Chem.* **1995**, *394*, 199.

DOI: 10.1021/jacs.6b08534
J. Am. Chem. Soc. 2016, 138, 13802−13805